LAUTECH JOURNAL OF ENGINEERING AND TECHNOLOGY 3(2) 2005: 99– 104

DEFECT SEGMENTATION TECHNIQUES FOR CERAMIC WALL TILE

D.O, Aborisade[1], and T. S Ibiyemi[2]

[1]Department of Electronics Engineering, Ladoke Akintola University of Tech., Ogbomoso, Oyo-state.

[2]Department of Electrical Engineering, University of Ilorin, Ilorin, Kwara-state

Abstract

This paper discussed the image processing algorithms that can be used to segment defects from the acquired ceramic tiles image. The paper proposed two gray-level threshold algorithms, a fixed threshold algorithm and an adaptive interpolating threshold algorithm. The two thresholding algorithms are tested across a set of test images and their performance compared using the area under receiver operator characteristic curves. The experimental results showed that the fixed threshold algorithm produces the receiver operator characteristic curve that encloses the greatest area and provides promising results in preference to the adaptive threshold algorithm.

INTRODUCTION

Automation of inspection and segmentation of the occurring defect on the industrial goods has gained importance with the recent developments on computer vision technologies. One can find recent researches on the subject, since the problem involves application of the computer vision and image processing methods [1, 2]. Some of the most common and anti-aesthetic defects found on some industrial goods are cracks, bumps, depressions, pin-holes, dirt, drops, and ondulations [3, 4, 5, 6].

This paper discussed the image processing algorithms that can be used to segment defects from the acquired ceramic tiles image. The paper commences in Section 2 by proposing the use of two gray-level thresholding techniques which are concerned with classifying pixels into object or background classes [7, 8, 9]. Section 3 presents performance evaluation methods and parameter setting of the algorithm. Simulation Results of the algorithm is discussed in Section 4. The paper ends in Sections 5 with some conclusion.

IMAGE THRESHOLDING

Surface microstructure defects in any manufactured item could be in millimeter and difficult to be detected and segmented by human operator using unaided manual techniques. In solving defect segmentation problem in this paper the reflective properties of the item surfaces is employed. As a case study the reflectance of the defect in ceramic tile image is much higher than that of the background [4]. This leads to strong contrast between background and defect in well illuminated images captured by the camera. The enhanced contrast makes the use of a gray level thresholding a viable background / defect segmentation technique. Defects from the capture tile image are simply extracted by means of the value of gray level. The purpose of gray level thresholding is to extract pixels which represent objects from the background of the image.

Two algorithms are proposed in this paper for segmenting defect from background on the basis of image grey-level value. The first algorithm is a straightforward threshold on the gray-level. The value of the output pixel g(x, y) is given by

$$g(x,y) = \begin{cases} 255 & for\ f'(x,y) \geq \tau \\ 0 & for\ f'(x,y) < \tau \end{cases} \qquad (1)$$

where $f'(x, y)$ is the corresponding pixel from the input image and τ is the threshold setting used to distinguish defects from the background. According to equation (1), bright pixels above or equal to the threshold are labeled white as defect, whilst the duller pixels less than the threshold are labeled black, as background.

However, in the case that the illumination over the ceramic image is different, owing to the nonuniformly distributed light condition which are common in industrial plants, the result can be that the objects in certain parts of the image may be lighter or darker than any other part. Therefore, it is inadequate to apply a single threshold to the whole image. If a single threshold is not acceptable, then the remaining option consists of using a number of different localized thresholds over small subregions of the image. This method decides threshold value based on the local

properties of the image. Several approaches have been proposed for this localized thresholding method [10, 11, 12]. The intensity gradient based thresholding method [10] use the linear approximation of the gradient as a measure of decision for the local threshold. The adaptive interpolating thresholding algorithm is expressed as follows:

$$g(x,y) = \begin{cases} 255 & for\ f^1(x,y) \geq \alpha\mu(y) \\ 0 & for\ f^1(x,y) < \alpha\mu(y) \end{cases} \quad (2)$$

where $g(x, y)$ is the output pixel, μ is the mean gray-level computed for both the top (μ_1) and bottom (μ_2) halves of the image and α is a gain that is used to set the threshold level.

To test the effectiveness / performances of the fixed and adaptive thresholding algorithms across a set of test images, ground truth labeling was produced for each set of test image by segmenting image pixels into defect and background using standard image editing software.

EVALUATION OF THE SEGMENTATION ALGORITHM

In assessing the utility of grey-level thresholding, receiver operator characteristic, ROC, curves were used [13, 14]. The area under the ROC curve reflects the discriminatory power of the thresholding algorithm taking the reflective surface property of the tiles into consideration.

Using gray-level as a discriminant between the two populations, Mann-Whitney statistic has been shown to be equivalent to the area underneath an ROC curve [15]. In the two class discrimination problems, the defect and background pixels are considered positive and negative, respectively. Both classes are characterized by the pixel gray-level, g_P and g_N, over the population of positives and negatives. In the case of discrete data, Mann-Whitney statistic is computed from a set of comparison scores [15]. Compare each pair of pixels g_P and g_N, the comparison scores is as follows

$$S(g_P, g_N) = \begin{cases} 1\ if\ g_P > g_N \\ \frac{1}{2}\ if\ g_P = g_N \\ 0\ if\ g_P < g_N \end{cases} \quad (3)$$

Therefore, for a set of n_p positive examples and n_N negatives Whitney statistic is written as

$$W = \frac{1}{n_P \bullet n_N} \sum_{1}^{n_P} \sum_{1}^{n_N} S(g_P, g_N) \quad (4)$$

This statistic is equivalent to area under ROC curve θ as demonstrated in Hanley and McNeil [15]. This is written as

$$\theta = W = P(g_P > g_N) \quad (5)$$

The equivalence arises from the fact that both quantities measure the probability that in randomly paired background and defect pixels, the gray-levels will allow the two pixels to be correctly identified.

In controlling the pixel classification, ROC curve is produced by varying the threshold as applied to the test image. At each setting, every pixel is placed into one of four groups:

1. True Positives (TP): defect pixels correctly classified as defect.
2. False Positives (FP): background pixels incorrectly classified as defect.
3. True Negatives (TN): background pixels correctly classified as background.
4. False Negatives (FN): defect pixels incorrectly classified as background.

Probability of classifying a positive (defect pixel) correctly at a threshold setting is given by

$$TPR = \frac{number\ TP}{number\ of\ TP + number\ of\ FN} \quad (6)$$

also probability of classifying a negative (background pixel) incorrectly at the same setting is given by

$$FPR = \frac{number\ FP}{number\ of\ FP + number\ of\ TN} \quad (7)$$

where TPR and FPR are the true positive ratio and false positive ratio, respectively, and both lie in the range (0, 1).

For each threshold setting, a (TPR, FPR) pair is generated which are plotted against each other to form the receiver operator characteristic (ROC) curve. The curve when generated over a range of algorithm parameter settings reflects the ability of the algorithm to perform segmentation task.

SEGMENTATION EXPERIMENTS – RESULTS

Images captured from four defective ceramic tiles given in Figure 1(a)-(d) are used for off-line testing of segmentation algorithms. Figure 2 shows the ROC curves generated for the adaptive interpolating threshold algorithm and the fixed threshold algorithm on each of the four data sets. Each curve was generated using 20 parameter settings; 20 settings of the gain α for the adaptive interpolating threshold algorithm, 20 settings of the threshold, τ for the fixed threshold algorithm.

The area under each ROC curve when calculated using the trapezium rule is given in Table 1.1, presented to the 4th decimal place.

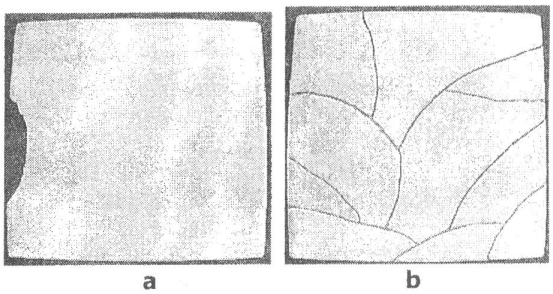

a b

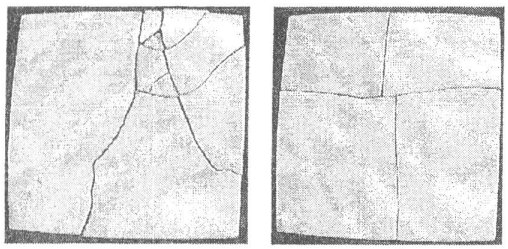

c d

Fig. 1: Gray-level images a – d for four defective ceramic wall tiles

Inspection of the figure in Table 1.1 and of the curves in Figure 2 shows that for gray-level images a – d, the performances of the adaptive interpolating threshold algorithm and fixed threshold algorithm are similar. However, the fixed threshold algorithm produces the ROC curve that encloses the greatest area and hence provides the better segmentation performance for a range of threshold or decision parameter settings than the adaptive threshold algorithm.

An approach to fixed threshold selection involves analyzing the gray-level histogram of the inspected image. Figure 3 (b) shows the gray-level histogram of each of the images in Figure 1 through which the thresholding value was generated. The result of the thresholding operation on each image following Sobel, Kirsch, and Prewitt edge enhancement operation are shown in Figure 3(c)-(e).

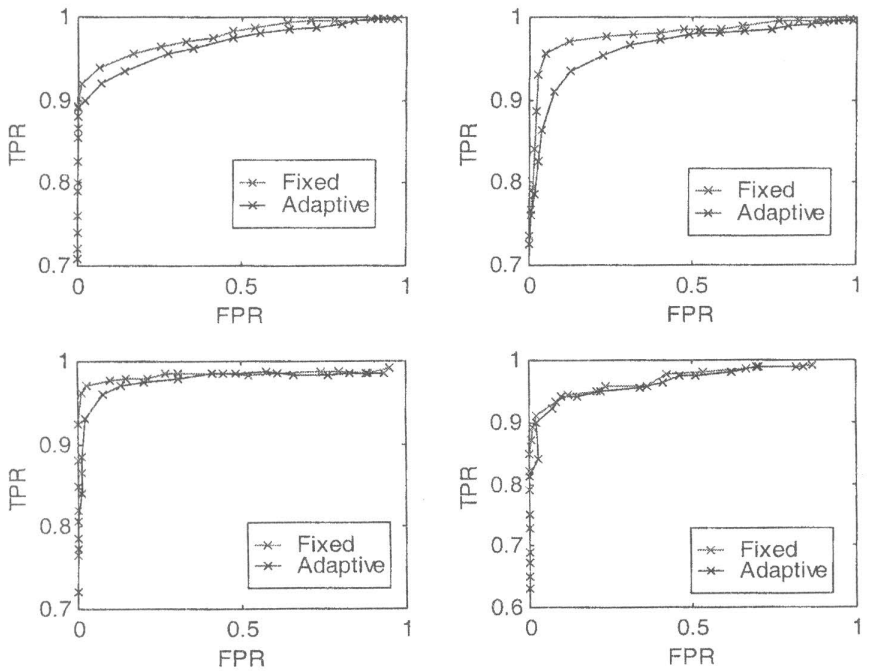

Fig. 2: ROC curves experimental results data sets a-d.

Table 1.1: Area underneath ROC curves for the fixed threshold and adaptive interpolating threshold algorithms for data sets a – d.

Data Set	Fixed	Adaptive
a	0.9651	0.9632
b	0.9852	0.9521
c	0.9915	0.9876
d	0.9234	0.9219

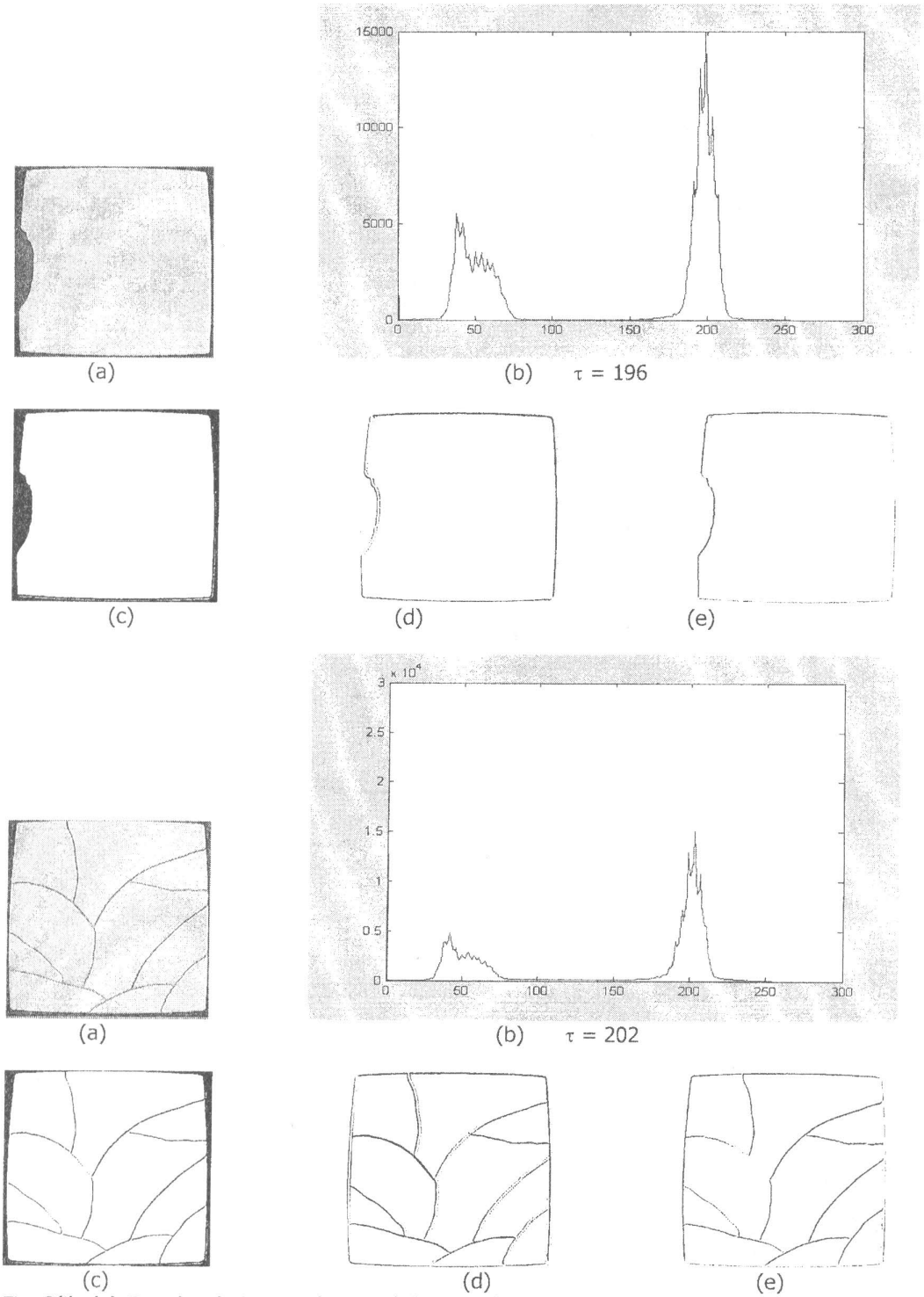

Fig. 3(i): (a) Gray-level picture of some defective tiles.
(b) Intensity histogram. (c, d and e) show the results obtained by thresholding the Sobel, Kircsh and Prewitt edge picture respectively.

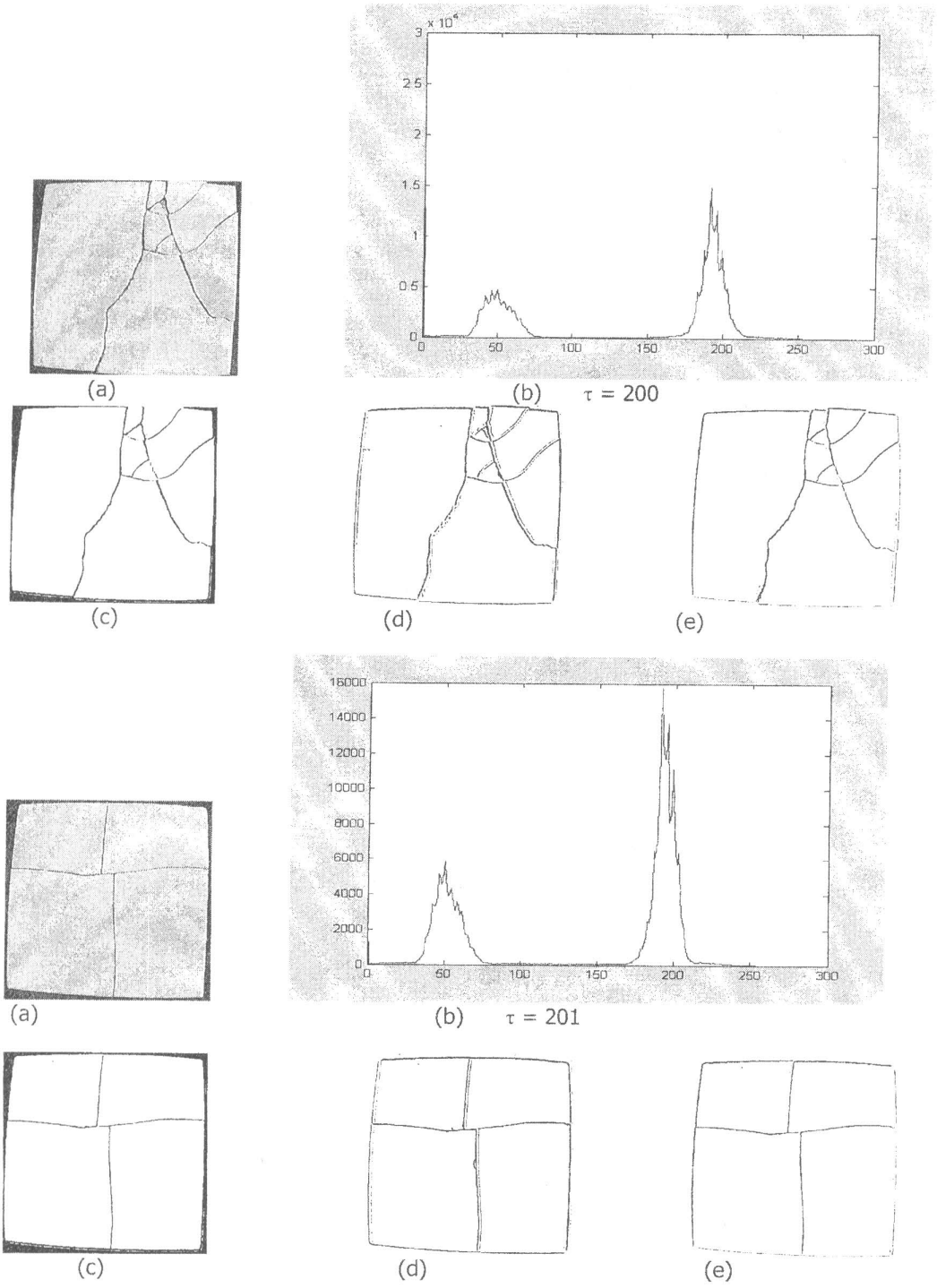

Fig. 3(ii): (a) Gray-level picture of some defective tiles.
(b) Intensity histogram. (c, d and e) show the results obtained by thresholding the Sobel, Kircsh and Prewitt edge picture respectively.

CONCLUSIONS

Two gray-level thresholding algorithms are presented in this paper for the extraction of defects from the surface of ceramic tiles image. The performance of the algorithms when tested on a limited number of test images using receiver operating characteristic curves produces encouraging results.

However, in the final analysis, fixed thresholding algorithm was shown to produce ROC curve that encloses the greatest area and provides the better segmentation performance for a range of threshold or decision parameter settings in preference to the adaptive threshold algorithm.

REFERENCES

Boukouvalas, C., Kittler, J., Marik, R., and Petrou, M., (1994). Automatic grading of ceramic tiles using machine vision, IEEE International Symposium on Industrial Electronics, pp. 13 – 18.

Davies, E. R., (2000). Image Processing: Low-level vision requirements, Electronics Communication Engineering journal, 12 (5):197 – 210.

Aborisade, D. O., (2005). A Development of Computer Vision for Real-Time Industrial Inspection, PhD thesis, Department of Electrical Engineering, University of Ilorin.

Bukouvalas, C., et al., (1995). Ceramic Tile Inspection for Colour and Structural Defects, Proceedings of the International Conference on Advances in Materials and processing Technologies.

Suresh, B. R, Fundakowski, R. A., Levitt, T. S., and Overland, J. E., (1983). A Real-Time Automated Visual Inspection System for Hot Steel Slabs, IEEE Trans. on PAMI, 5(6): 563 – 572.

Sun, H., Xu, K., and Xu, J., (2003). Online Application of Automatic Surface Quality Inspection System to finishing line of Cold Rolled Strips, Journal of University of Science and Technology, Beijing, 10 (4): 38 – 41.

Fu, K. S. and Mui, J. K., (1981). A survey on image segmentation, Pattern Recognition, 13: 3 – 16.

Sahoo, P. K., Soltani, S. and Wong, A. K. C., (1988). A survey of thresholding techniques, Computer Vision, Graphics and Image Processing, 41: 233 – 260.

Joan S. W., (1978). A survey of threshold selection techniques, Computer Graphics and Image Processing, 7: 259 – 265.

Parker, J. R., (1991). Gray level thresholding in badly illuminated images, IEEE Trans. Pattern Anal. Machine Intell., 13: 813 – 819.

Lie, W. N., (1995). Automatic target segmentation by locally adaptive image thresholding, IEEE Trans . Image Processing, 4: 1036 – 1041.

Vinod, V., and Chaudhury, S., (1993). A connectionist approach for gray level image segmentation, in Proc. 11th IAPR Int. Conf. Pattern Recognition, 3: 489 – 492.

Green, D. M. and Swets, J. A., (1996). Signal Detection Theory and Psychophysics, John Wiley and Sons.

Van Trees, H. L., (1968). Detection, Estimation and Modulation Theory, Part I, John Wiley and Sons.

Hanley, J. A. and McNeil, B. J., (1982). The meaning and use of the area under a receiver operating characteristic (ROC) curve, Radiology, 143: 29 – 36.